Electronic quasiparticles in the quantum dimer model: Density matrix renormalization group results

Electronic quasiparticles in the quantum dimer model: density matrix renormalization group results

Junhyun Lee,[1] Subir Sachdev,[1,2] and Steven R. White[3]

[1]*Department of Physics, Harvard University, Cambridge MA 02138, USA*

[2]*Perimeter Institute for Theoretical Physics, Waterloo, Ontario, Canada N2L 2Y5*

[3]*Department of Physics and Astronomy, University of California, Irvine, CA 92697-4575 USA*

(Dated: June 15, 2016)

Abstract

We study a recently proposed quantum dimer model for the pseudogap metal state of the cuprates. The model contains bosonic dimers, representing a spin-singlet valence bond between a pair of electrons, and fermionic dimers, representing a quasiparticle with spin-1/2 and charge $+e$. By density matrix renormalization group calculations on a long but finite cylinder, we obtain the ground state density distribution of the fermionic dimers for a number of different total densities. From the Friedel oscillations at open boundaries, we deduce that the Fermi surface consists of small hole pockets near $(\pi/2, \pi/2)$, and this feature persists up to doping density 1/16. We also compute the entanglement entropy and find that it closely matches the sum of the entanglement entropies of a critical boson and a low density of free fermions. Our results support the existence of a fractionalized Fermi liquid (FL*) in this model.

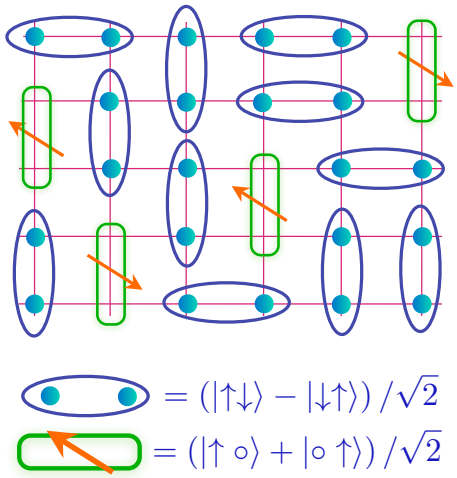

FIG. 1. A state in the Hilbert state of the dimer model. The blue dimers are bosons representing a spin-singlet pair of electrons. The green dimers are spin 1/2 fermions representing an electron in a bonding orbital between a pair of sites.

I. INTRODUCTION

A recent paper [1] has proposed a simple quantum dimer model for the pseudogap metal state of the hole-doped cuprates. The objective of this model is to describe a metal with electron-like quasiparticles, carrying spin 1/2 and charge e, but with a Fermi volume which violates the Luttinger theorem for a Fermi liquid (FL). In particular, doping a density of p holes away from a half-filled insulator should yield, in Fermi liquid theory, a hole Fermi surface of size $1 + p$. And indeed, just such a Fermi surface is observed at large p [2]. However, for $p \approx 0.1$, in the pseudogap metals, many physical properties are well described by a model of electron-like quasiparticles with a Fermi surface of size p [3]. Such a Fermi surface can be obtained in a 'fractionalized Fermi liquid' (FL*) [4, 5]. The model of Ref. [1] was designed to yield a FL* state with a Fermi surface of size p using ingredients that are appropriate for a single-band model of cuprate physics.

Our paper will present density matrix renormalization group (DMRG) results on the dimer model. The exact diagonalization results in Ref. [1] were limited to a lattice size of 8×8 and a single fermionic dimer. Here we study significantly larger systems with up to 8 fermions, and obtain results on the density distribution of the fermionic dimers and the entanglement entropy. As we shall see below, all of our results are consistent with the appearance of a FL* metal in this dimer model.

II. MODEL AND DMRG SETUP

The quantum dimer model of Ref. [1] has bosonic dimers and spin 1/2 fermionic dimers, which close pack a square lattice with an even number of sites: see Fig. 1. The bosonic sector of this model is identical to that of the original study of Rokhsar and Kivelson (RK) [6], with potential and resonating term for dimers within a plaquette. In addition, fermionic dimers may move via hopping terms whose form will be specified below. Interaction between the fermionic dimers can in principle be present, but are not expected to be important when the density of fermions is low; we will not include fermion-fermion interactions here.

Now we state the Hamiltonian for this model. Let us first define the operators creating (annihilating) bosonic and fermionic dimers as $D^\dagger_{ix}(D_{ix})$ and $F^\dagger_{ix\alpha}(F_{ix\alpha})$, respectively. The extra indices i and $x(y)$ indicates the created or annihilated dimer resides on the link between $i = (i_x, i_y)$ and $i + \hat{x}(\hat{y})$, where $\hat{x} = (1, 0)$ and $\hat{y} = (0, 1)$ are unit vectors and $\alpha =\uparrow, \downarrow$ is spin index. Note that we set the lattice spacing to 1. In the language of the t-J model, D and F operators have the following correspondence to the electron creation and annihilation operators $c^\dagger$, c,

$$\begin{aligned} D^\dagger_{i\eta} &\sim \frac{(-1)^i}{\sqrt{2}} \left(c^\dagger_{i\uparrow} c^\dagger_{i+\hat{\eta},\downarrow} + c^\dagger_{i\downarrow} c^\dagger_{i+\hat{\eta},\uparrow} \right), \\ F^\dagger_{i\eta\alpha} &\sim \frac{(-1)^i}{\sqrt{2}} \left(c^\dagger_{i\alpha} + c^\dagger_{i+\hat{\eta},\alpha} \right). \end{aligned} \tag{2.1}$$

$(-1)^i$ is due to a gauge choice which we follow from Ref. [6]. We can observe that the quantum numbers of states $D^\dagger_i|0\rangle$ and $F^\dagger_{i\alpha}|0\rangle$ are the same as $c^\dagger_{i\uparrow}c^\dagger_{i\downarrow}|0\rangle$ and $c^\dagger_{i\alpha}|0\rangle$, setting aside the fact that the degrees of freedom of the former lives between two sites (i and $i+\hat{\eta}$) and the latter resides on each site. This fact will be useful in our DMRG setup. We can now write the Hamiltonian for the model in terms of dimer creation and annihilation operators, [1]

$$\begin{aligned} H &= H_{\rm RK} + H_1 \\ H_{\rm RK} &= \sum_i \Big[-J\, D^\dagger_{ix} D^\dagger_{i+\hat{y},x} D_{iy} D_{i+\hat{x},y} + 1 \text{ term} \\ &\qquad + V\, D^\dagger_{ix} D^\dagger_{i+\hat{y},x} D_{ix} D_{i+\hat{y},x} + 1 \text{ term} \Big] \\ H_1 &= \sum_{i,\alpha} \Big[-t_1\, D^\dagger_{ix} F^\dagger_{i+\hat{y},x\alpha} F_{ix\alpha} D_{i+\hat{y},x} + 3 \text{ terms} \\ &\qquad - t_2\, D^\dagger_{i+\hat{x},y} F^\dagger_{iy\alpha} F_{ix\alpha} D_{i+\hat{y},x} + 7 \text{ terms} \\ &\qquad - t_3\, D^\dagger_{i+\hat{x}+\hat{y},x} F^\dagger_{iy\alpha} F_{i+\hat{x}+\hat{y},x\alpha} D_{iy} + 7 \text{ terms} \\ &\qquad - t_3\, D^\dagger_{i+2\hat{y},x} F^\dagger_{iy\alpha} F_{i+2\hat{y},x\alpha} D_{iy} + 7 \text{ terms} \Big]. \end{aligned} \tag{2.2}$$

The terms we have not explicitly written down are connected with the previous term through a symmetry transformation of the square lattice. $H_{\rm RK}$ is the pure bosonic sector mentioned above; J is the coupling for the resonant term, and V is the coupling for the potential term. H_1 contains the hopping terms of the fermionic dimers; t_1, t_2, and t_3 correspond to three distinct types of hoppings.

In the absence of the fermions, the undoped dimer model has an exactly solvable point (the RK point) at $V = J$, with a spin liquid ground state given by the equal superposition state of all allowed D_i dimer configurations [6]. But away from this point, bipartite dimer models are described by a dual compact U(1) gauge theory [7], and have been argued to have only confining valence bond solid ground states [8–10]. Once we add a finite density of fermions, it is expected that generic dimer models of the form in Eq. (2.2) on bipartite lattices have confining valence bond solid ground states [11]. However, the confinement length scale is large near the RK point and at small fermion density, and a spin-liquid FL* state should be effectively realized when the confinement scale is larger than the system size. We study such a regime in the present paper, and for our system sizes, our results are consistent with deconfinement.

In our DMRG calculation, we consider a lattice with geometry of a finite cylinder. The circumference of the cylinder consists of four lattice sites, and the length of the cylinder is up to 32 sites. In the second part of this paper, we also compute entanglement entropies in 64×2 cylinder to observe one-dimensional effects. We repeat our calculation in different fermionic dimer densities, from one to 8 fermionic dimers. Note that in our lattice configuration, 8 fermionic dimers correspond to 1/16 doping in the typical cuprate phase diagram. We use two sets of parameters for the couplings in Eq. (2.2). One is the parameters which is relevant to the physical model for the cuprates in the pseudogap regime: $t_1 = -1.05J$, $t_2 = 1.95J$, and $t_3 = -0.6J$, near the RK point ($V = 0.9J$). The other is the parameter which we choose for comparison: $t_1 = t_2 = t_3 = J$, also with $V = 0.9J$. The single fermion study in Ref. [1] suggests the different hopping parameters change the dispersion of the fermionic dimer: the Fermi surface consists of four hole pockets near $(\pm\pi/2, \pm\pi/2)$ in the former parameter regime, and a single Fermi surface centered at $(0, 0)$ in the latter. We will confirm this behavior in our DMRG calculation below, while studying a multiple fermion system.

The fact that we are interested in observing the hole pockets, is closely related to the reason we chose the circumference as four lattice site for the first part of our calculation. The center of the four hole pockets are at $\vec{k} \sim (\pm\pi/2, \pm\pi/2)$, and the minimum number of sites in y-direction needed to get information about $k_y = \pm\pi/2$ is four. This is why we could not choose two sites in the circumference when our focus is in the fermion dispersion. Later when we concentrate on the one-dimensional scaling properties of the entanglement entropies, we study the case of a cylinder of two sites along the circumference, which allows us to calculate much longer system.

Now we comment on the topological sectors of the Hamiltonian. The Hilbert space we are considering consists of closely packed configurations of dimers. For each configuration, we can define an integer quantity

$$w_x = \sum_{i_x=1}^{N_x} (-1)^{i_x} (D^\dagger_{(i_x,i_y)y} D_{(i_x,i_y)y} + F^\dagger_{(i_x,i_y)y\alpha} F_{(i_x,i_y)y\alpha}), \tag{2.3}$$

for any $1 \leq i_y \leq N_y$, where $N_x(N_y)$ is the number of sites in the $x(y)$ direction and the spin α implicitly summed. One can observe that every term in Eq. (2.2) preserves this quantity, so the possible configurations of the dimers spanning the Hilbert space can be divided in different sectors with different values of w_x. The integer w_x is the topological winding number associated with loops in the transition graph that circles the x-axis, similar to that of the RK model on a torus [6]. The integer w_y can be defined in an analogous manner, but it is not meaningful since we do not have periodic boundary condition in x-direction. In principle, we would like to restrict ourselves in the zero winding number sector, $w_x = 0$. Right at the RK point, $J = V$, each topological sector has a unique ground state with zero energy, which is an equal superposition of all configurations [6]. Since the number of configurations are largest at $w_x = 0$, sectors with large absolute value of w_x have lower entanglement and will be preferred by DMRG. One way of imposing the $w_x = 0$ condition is to add a potential term proportional to w_x^2 to the Hamiltonian, at the price of more computation. Another method is to tune V to be slightly smaller than J and penalize states moving away from $w_x = 0$. In this case, the amount of computation is similar to that without the constraint, because we do not add any additional terms to the Hamiltonian. However, we have to choose an optimal value for the V/J. We adopt the latter method, since moving away from the fine-tuned RK point is beneficial for us, and in all of our calculations, we have used $V = 0.9J$. The confinement length scales are large enough at this coupling so that we don't observe valence bond solid order, even in the undoped case.

Each bond in the square lattice can have four states: occupied by a bosonic dimer, occupied by a spin up or down fermionic dimer, or empty. As mentioned previously, one useful observation is that the quantum numbers of the bonds are the same as the quantum numbers of the sites in a spin-half fermion model, with the bosonic dimer occupied state corresponding to the filled (spin up and down) state. Therefore we can map our dimer model to a fermionic Hubbard model on the links, with dimer constraints. The dimer constraint is to ensure each site is part of only one dimer, and this is achieved in our DMRG as an additional potential term. We use a potential of $\sim 20J$ to penalize overlapping dimers.

All DMRG calculations in this paper were performed with the ITensor library [12]. We kept up to ~ 600 states to keep the truncation error per step to be $\sim 10^{-8}$.

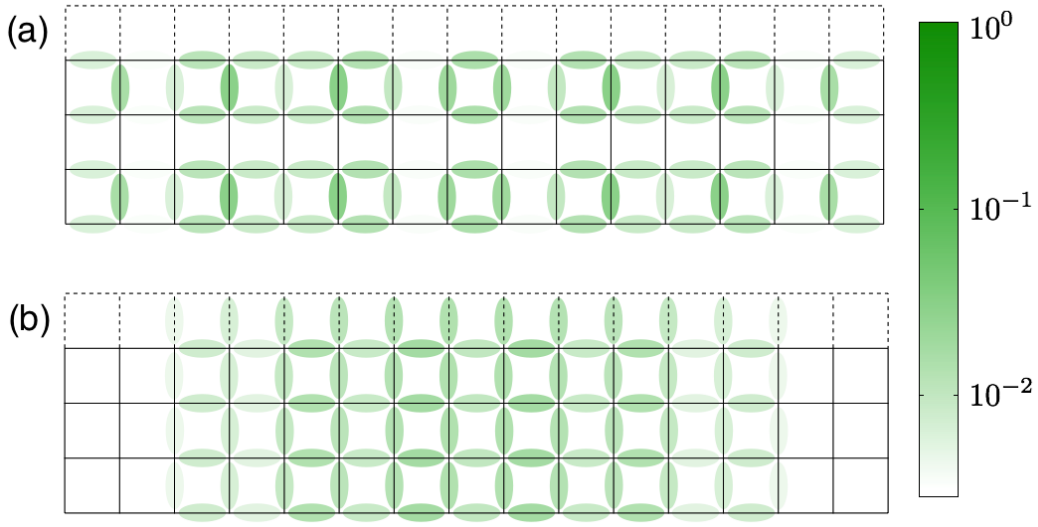

FIG. 2. The log scale density of fermionic dimers on a 16×4 lattice. The configuration consists with a single fermionic dimer and 31 bosonic dimers. The dashed line indicates the periodic boundary condition in the y-direction; the top dashed line is identified to the bottom solid line. The hopping parameters used are (a) $t_1 = -1.05J$, $t_2 = 1.95J$, $t_3 = -0.6J$; (b) $t_1 = t_2 = t_3 = J$. In (a), one can observe the density oscillation with period of roughly two lattice sites, which corresponds to crystal momenta of $\pi/2$. Note that the Hilbert space is closely packed dimer configuration, and sites without fermionic dimers are occupied by bosonic dimers.

III. DENSITY MODULATION

Now we show the results of the DMRG calculations where we can observe the change in dispersions with different hopping parameters, and especially the existence of a dispersion with Fermi pockets centered near $\vec{k} = (\pm\pi/2, \pm\pi/2)$. Extracting momentum information from DMRG is not trivial since it is a real-space calculation. (For few fermions, one can use techniques used in Ref. [13] to achieve this. Also, there are more recent schemes for DMRG in mixed real and momentum space proposed in Ref. [14]). However, we may observe Friedel oscillations from the open boundaries of our system, and these will reveal information of the fermionic dimer's momentum in the cylinder direction.

First we check whether the Friedel oscillation observed in the case of a single fermionic dimer is consistent with Ref. [1]. Fig. 2 is the density profile of the fermionic dimers when a single fermionic dimer is present among bosonic dimers on a 16×4 lattice, for the two parameter sets we use. From Fig. 2 (a), which is the parameter set expected to have hole pockets, we can observe an oscillation of the profile starting from the open boundary to the x-direction. This is especially

clear when looking at the vertical dimers. The period of the oscillation is roughly two lattice sites. Since the Friedel oscillation has a wavevector of $2k_F$, this indicates that the fermionic dimer in the ground state has crystal momentum of $k_x \sim \pi/2$. This fact is consistent with the exact diagonalization study in Ref. [1], which found the energy minima of the single fermion spectrum to be near $\vec{k} = (\pi/2, \pi/2)$. On the other hand, Fig. 2 (b) does not show any prominent oscillation near the boundary. This calculation has been done with the parameters which is expected to have a single band with the dispersion minima at $\vec{k} = (0, 0)$, so the absence of Friedel oscillation is expected. We have performed the same calculation for a single fermionic dimer while increasing the x-direction of lattice size, up to 32×4 lattice and observed the same behavior, in both cases with dispersion minima at $k_x = \pi/2$ (Fig. 2a) and $k_x = 0$ (Fig. 2b). A more quantitative analysis for the 32×4 lattice by Fourier transform will follow below, together with the higher density calculation.

Note that Fig. 2a seems to break the translation symmetry in the y-direction. However, this is just a spontaneous symmetry breaking between the two degenerate ground states; one being Fig. 2a and the other being Fig. 2a translated by one lattice site in the y-direction. One can check this by computing the ground state several times and obtaining both states, or by adding a small perturbation acting as a chemical potential on vertical bonds with particular y-coordinate, and observing the absence of the symmetry. The fact that Fig. 2b does not break the symmetry is also in accordance with our claim. Since the state of Fig. 2b has only one Fermi surface centered at $\vec{k} = (0, 0)$, there is no degeneracy in the ground state.

We would like to study the Friedel oscillation more quantitatively and verify whether this feature survives when we increase the number of fermionic dimers, n. We keep the lattice size as 32×4 and increase n up to 8, which corresponds to $1/16$ doping. Since the 'defects' of the system are the open boundaries, the Friedel oscillation is in the cylinder direction. From the density profile $\rho(x, y)$, we define $\rho_x(x) = \sum_y \rho(x, y)$ and perform Fourier transformation. The result is shown in Fig. 3. Note that we have normalized the data by $1/n$, and the magnitude 1 peak at $k_x = 0$ indicates the total density is n. Other than the $k_x = 0$ peak, we can observe that there is a peak at $k_x = 7\pi/8$ in $n = 1, 3, 4, 5$ of Fig. 3a, where the parameter set used is the same as Fig. 2 (a). This peak is due to the Friedel oscillation, and indicates that $k_x = 7\pi/16$ at the Fermi level. Ref. [1] showed the energy minimum is at $\vec{k} = (q, q)$ for q slightly less than $\pi/2$, and this is in good agreement with our result. Based on experiments and previous works one can argue the energy minimum should be either at the origin ($\vec{k} = (0, 0)$) or along the diagonal ($\vec{k} = (q, q)$). Therefore, we can conclude the dispersion of the dimer model in our cylinder will have a minimum at $\vec{k} = (7\pi/16, \pi/2)$, and in the large system limit this will converge to a diagonal point $\vec{k} = (q, q)$ with $7\pi/16 \leq q \leq \pi/2$. Moreover, from $n = 7, 8$ data of Fig. 3a, we can observe the expansion of the Fermi surface as we increase the fermionic dimer density. The new peak at $k_x = 13\pi/16$ indicates that the Friedel

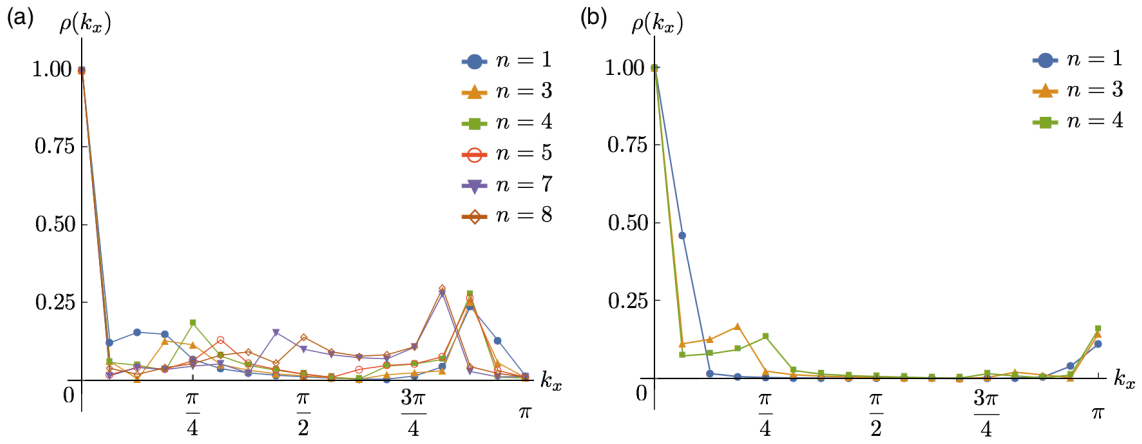

FIG. 3. Fourier transform of the density of fermionic dimers with various total densities. n denotes the number of fermionic dimers in the system. Note that in our 32×4 lattice, $n = 8$ corresponds to $1/16$ doping. The hopping parameters used are (a) $t_1 = -1.05J$, $t_2 = 1.95J$, $t_3 = -0.6J$; (b) $t_1 = t_2 = t_3 = J$. In (a), there are peaks at $13\pi/16$ and $7\pi/8$ which indicates the fermionic dimer with $k_x = 13\pi/32$ and $7\pi/16$ are at the Fermi level, which is a feature missing in (b). The central peak at 0 is due to the total density and is normalized to 1.

oscillation is now from the new Fermi level at $k_x = 13\pi/32$.

For Fig. 3b, which used the same parameter set as Fig. 2 (b), there is no peak at $k_x = 7\pi/8$ for any n. This is in accordance with our expectation that the state has dispersion minimum at $\vec{k} = (0, 0)$, and also with the qualitative result we have seen in Fig. 2 (b). There is a signal at $k_x = \pi$, however the origin of this signal is not the Friedel oscillation. Fig. 4 shows the density of the fermionic dimer as a function of x. The plotted one-dimensional density $\rho(x) = \sum_y \rho(x, y)$ is the Fourier transform of $\rho(k_x)$, which is the quantity plotted in Fig. 3. The x-axis of the plot is the position in the unit of lattice constant. Integer values are for the vertical bonds and half-integers are for the horizontal bonds. Looking at only the vertical bonds does not show any modulation in the density and looks very much like a particle in a box. On the other hand, the horizontal bond shows some modulation with two lattice sites. This density modulation clearly has a wavevector of π, and is the reason of the signal at $k_x = \pi$ in Fig. 3b. Although the precise reason for this oscillation is unclear, we can clearly see that this modulation is present throughout the bulk and the signal at $k_x = \pi$ does not indicate Friedel oscillation from $k_F = \pi/2$: it appears to be simply a lattice commensuration effect.

Note that we have not included the data obtained for n which $\mathrm{mod}\,(n, 4) = 2$. The calculations with such n had a stronger tendency towards $w_x \neq 0$ topological sector, and we had to decrease V further to keep the state in $w_x = 0$. (For $n = 2$, we needed $V < 0.8$) This seems to be an artifact of our system which is effectively one-dimensional and can only have four values of k_y.

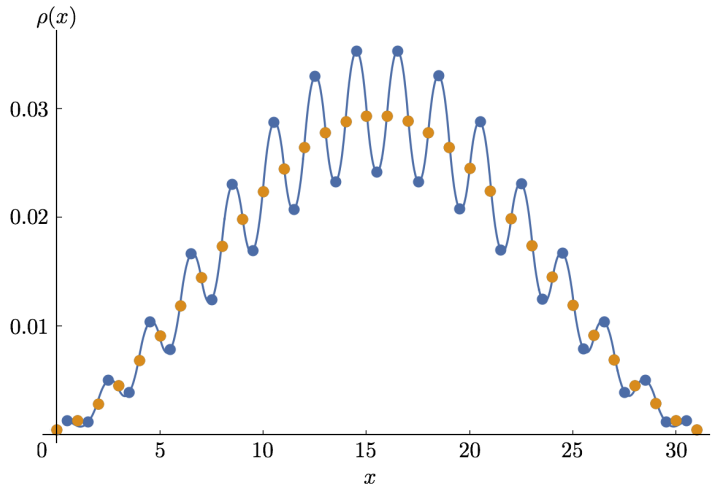

FIG. 4. One dimensional plot for fermionic dimer density ($\rho(x) = \sum_y \rho(x, y)$) as a function of distance in x direction, when $n = 1$. The x-axis unit is the lattice constant. Vertical bonds have integer x and colored yellow; horizontal bonds have half-integer x and colored blue. Notice the modulation is only present in the horizontal dimers. The system is a 32×4 cylinder with parameters $t_1 = t_2 = t_3 = J$.

IV. ENTANGLEMENT ENTROPY

We present the result for the computation of Rényi entropy to gain more information about the ground state of the dimer model. First recall the definition of the α-th Rényi entanglement entropy:

$$S_\alpha = \frac{1}{1-\alpha} \ln \left[\mathrm{Tr}\, \rho_A^\alpha \right]. \tag{4.1}$$

Here, ρ_A is the reduced density matrix of partition A, i.e. $\rho_A = \mathrm{Tr}_B\, \rho$, where $A \cup B$ is the total system. Note that α-th Rényi entropy becomes the von Neumann entropy in the $\alpha \to 1$ limit.

In a one-dimensional gapless system, conformal field theory (CFT) has a result for the scaling of the Rényi entropy: [15, 16]

$$S_\alpha = \frac{c}{12}\left(1 + \frac{1}{\alpha}\right) \ln\left(\frac{2L}{\pi} \sin\frac{\pi l}{L}\right) + g + c'_\alpha. \tag{4.2}$$

This is the case for a finite system of length L with open boundary condition, divided into two pieces which length of one piece is l. g is the boundary entropy [17], and c'_α is a non-universal constant. Considering our system as quasi-1D, we can extract the central charge c, of the system from this equation. For the entanglement entropy calculation, we consider both 32×4 and 64×2 cylinder to see any scaling behavior as the system approaches to one-dimension. Moreover, now we concentrate on the parameters which gives a single Fermi surface, $t_1 = t_2 = t_3 = J$. The results for the other

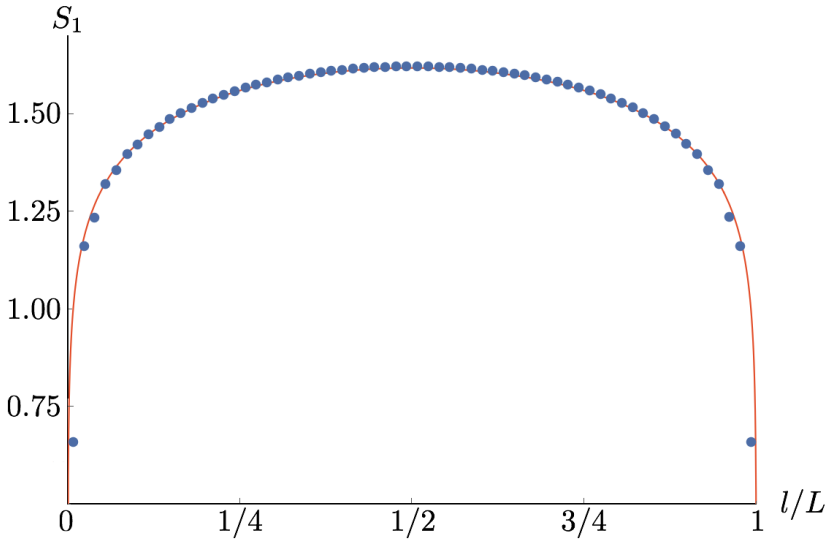

FIG. 5. von Neumann entropy of the pure RK model, calculated on a 64×2 cylinder. The red solid line is not the interpolation of the data points, but the exact CFT result of Eq. (4.2) with $c = 1$ and $g + c'_\alpha = 1$.

parameter are expected to be four copies of the presented results, in the thermodynamic limit. However, the density modulations resulting from the open boundaries prevent the entanglement entropy data having a nice one-dimensional scaling form for $L = 32$.

First we show the comparison of the von Neumann entropy of the pure RK model, with $n = 0$ fermions, with the CFT result (4.2) in Fig. 5. An excellent fit is found for $c = 1$. The fermion-free dimer model is dual to a sine-Gordon model [7, 8], and in 1+1 dimension this has a gapless phase described by a massless relativistic boson with $c = 1$. The results of Fig. 5 are in accord with this expectation.

Turning to the case with fermions, the von Neumann entropy with dispersion expected to have a single Fermi surface near $\vec{k} = (0, 0)$ is shown in Fig. 6. The results are for 64×2 lattice. Data for 32×4 lattice are not shown, but are very similar to the presented data (32×4 results are included in Fig. 7). We also include the data from Fig. 5 for the case without any fermions. It is clear that these is an additional contribution from the presence of the fermions, but it cannot be accounted for by changing the central charge of the CFT. Fermions at non-zero density in an infinite system should form a Fermi surface, and in the quasi-one dimensions geometry, each Fermi point should yield an additional contribution of $c = 1/2$ of a chiral fermion. It is clear that the data in Fig. 6 are not of this form.

Instead, we found that an excellent understanding of Fig. 6 is obtained by thinking about the limit of a very low density of fermions at the bottom of a quadratically dispersing band. This is the case of a "Lifshitz" transition in one dimension, when the chemical potential crosses the

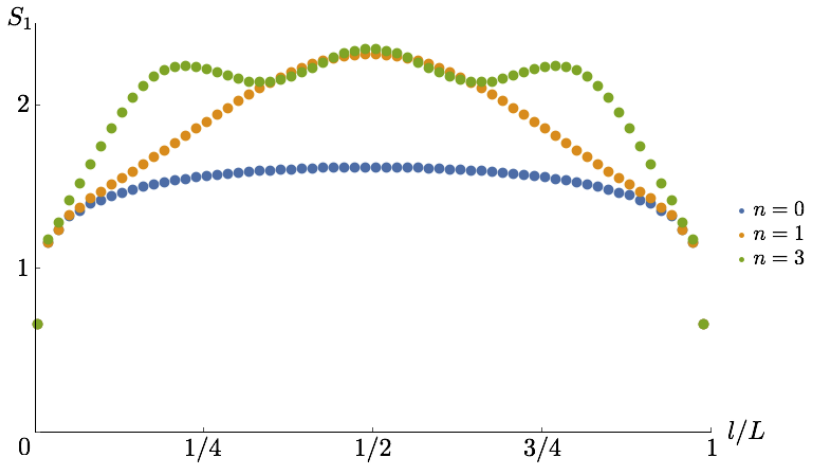

FIG. 6. von Neumann entropy of the FL* phase with different fermionic dimer densities. The system is a 64×2 cylinder with parameters $t_1 = t_2 = t_3 = J$. L is the length of the system, and l is the length of the subsystem. In the case of $n = 0$, which is a pure bosonic dimer model near the RK point, we get a nice fit to Eq. (4.2) with central charge 1.

bottom of a band. Ref. [18], studied the entanglement entropy near such a Lifshitz transition. In their Fig. 11, they present the entanglement entropy of a half-filled free fermion system with 200 sites, as the next-nearest hopping t is tuned to go across the Lifshitz transition. (The Hamiltonian used is $H = -\sum_i (c_i^\dagger c_{i+1} + t c_i^\dagger c_{i+2}) + \text{h.c.}$) Different graphs are labeled by different values of t, but basically what is changing is the number of occupied states above the Lifshitz transition. For example, when $t = 0.5$, only the large Fermi surface is occupied; when $t = 0.51$, the system has just gone through Lifshitz transition and one state is occupied from the new band; when $t = 0.52$, two states are occupied above the Lifshitz transition. The number of modulations in the entanglement entropy exactly matches the number of states filled above the Lifshitz transition.

We reproduced the data of Fig. 11 in Ref. [18] to compare with the behavior of the entanglement entropy with our own system of fermionic and bosonic dimers. Fig. 7 shows the fermionic contribution ΔS_1 of the entanglement entropy. This is obtained by subtracting the entanglement entropy of $n = 0$, which was shown in Fig. 5 to be due to a $c = 1$ boson field. To compare with the case of Lifshitz transition, we also subtract the entanglement entropy of the system with only one large band occupied, which is $t = 0.50$ in the specific model, from the system with one (three) state(s) occupied in the new band, corresponding to $t = 0.51$ (0.53); in this case, the gapless fermions from the occupied large band contribute as a $c = 1$ field. As seen in Fig. 7, ΔS_1 for $n = 1$ is nearly identical to the corresponding entanglement entropy for the Lifshitz transition for free fermions with two different lattice sizes. For $n = 3$, the value of ΔS_1 decreases slightly as the length of the system decreases, but the qualitative features remain the same. Note that in these

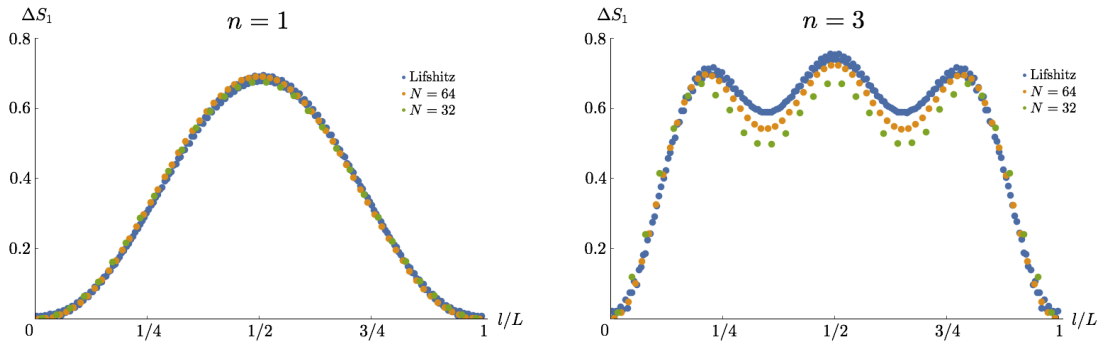

FIG. 7. Fermion contribution to von Neumann entropy of the dimer model and the Lifshitz transition. ΔS_1 equals $S_1(n = 1) - S_1(n = 0)$ in the left, $S_1(n = 3) - S_1(n = 0)$ in the right, where n is the number of fermionic dimers. The system is 64×2 and 32×4 cylinder with parameters $t_1 = t_2 = t_3 = J$ for the dimer model, and free fermions on a 200 site chain for the Lifshitz transition. The $n = 1$ and $n = 3$ cases for Lifshitz transition corresponds to the number of occupied state in the new band.

data, only the total length of the system was scaled to unity.

The above results provide strong evidence that the dimer model can be viewed as two approximately independent systems: a background $c = 1$ boson corresponding to the resonance between the dimers (both blue and green [11]), and a dilute gas (of density p) of free fermions. These are precisely the characteristics of the FL* state, which has an emergent gauge field (represented here by the $c = 1$ boson) and a Fermi surface of electron-like quasiparticles.

V. OUTLOOK

The combination of our results on the density distribution and the entanglement entropy confirm the expected appearance of a FL* state in the dimer model of Ref. 1. By general arguments [5, 19], the violation of the Luttinger theorem for a Fermi liquid requires that the emergent gauge fields appear in the spectrum of the theory. Our results on the entanglement entropy in a quasi-one-dimensional geometry are in accord with this requirement, showing a background $c = 1$ boson that is expected from the gauge theory of the dimer model [7, 8]; the boson represents the modes associated with the "resonance" between the dimers around a plaquette. Above this gauge field background, we obtained evidence for a gas of nearly-free fermions of density p, both in the density modulations and in the entanglement entropy: in particular, the fermionic contribution to the entanglement entropy closely matched that of a dilute gas of free fermions near the bottom of a quadratically dispersing band.

One possible direction to extend our work is to use the infinite-DMRG (iDMRG). By using iDMRG we will be able to compute correlation functions of all length scales, and can obtain mo-

mentum distribution and quasiparticle residue of Fermionic dimers. Still, our momentum resolution in k_y will be restricted by N_y.

Another approach is to use the recent proposal of DMRG in mixed real and momentum space [14]. By this method we will be able to determine k_y more directly, which can be evidence of the existence of the hole pockets. Moreover, Ref. [14] claims the computation time is reduced by more than an order of magnitude, so this may allow us to include more sites in y-direction (in this case, equivalently, more k_y points).

Acknowledgements

We thank A. Allais, M. Punk, B. Swingle, and W. Witczak-Krempa for useful discussions. JL is particularly grateful to M. Stoudenmire for introducing and teaching DMRG and ITensor library. The research was supported by the NSF under Grant DMR-1360789 (JL, SS) and DMR-1505406 (SRW) and MURI grant W911NF-14-1-0003 from ARO (JL, SS). Research at Perimeter Institute is supported by the Government of Canada through Industry Canada and by the Province of Ontario through the Ministry of Research and Innovation.

---

[1] M. Punk, A. Allais, and S. Sachdev, "A quantum dimer model for the pseudogap metal," Proc. Nat. Acad. Sci. **112**, 9552 (2015), arXiv:1501.00978 [cond-mat.str-el].

[2] M. Platé, J. D. Mottershead, I. S. Elfimov, D. C. Peets, R. Liang, D. A. Bonn, W. N. Hardy, S. Chiuzbaian, M. Falub, M. Shi, L. Patthey, and A. Damascelli, "Fermi Surface and Quasiparticle Excitations of Overdoped $Tl_2Ba_2CuO_{6+\delta}$," Phys. Rev. Lett. **95**, 077001 (2005), cond-mat/0503117.

[3] S. Sachdev and D. Chowdhury, "The novel metallic states of the cuprates: topological Fermi liquids and strange metals," ArXiv e-prints (2016), arXiv:1605.03579 [cond-mat.str-el].

[4] T. Senthil, S. Sachdev, and M. Vojta, "Fractionalized Fermi Liquids," Phys. Rev. Lett. **90**, 216403 (2003).

[5] T. Senthil, M. Vojta, and S. Sachdev, "Weak magnetism and non-Fermi liquids near heavy-fermion critical points," Phys. Rev. B **69**, 035111 (2004).

[6] D. Rokhsar and S. A. Kivelson, "Superconductivity and the Quantum Hard-Core Dimer Gas," Phys. Rev. Lett. **61**, 2376 (1988).

[7] E. Fradkin and S. A. Kivelson, "Short range resonating valence bond theories and superconductivity," Mod. Phys. Lett. B **04**, 225 (1990).

[8] N. Read and S. Sachdev, "Spin-Peierls, valence-bond solid, and Néel ground states of low-dimensional quantum antiferromagnets," Phys. Rev. B **42**, 4568 (1990).

[9] A. Vishwanath, L. Balents, and T. Senthil, "Quantum criticality and deconfinement in phase transitions between valence bond solids," Phys. Rev. B **69**, 224416 (2004).

[10] E. Fradkin, D. A. Huse, R. Moessner, V. Oganesyan, and S. L. Sondhi, "Bipartite Rokhsar Kivelson points and Cantor deconfinement," Phys. Rev. B **69**, 224415 (2004), cond-mat/0311353.

[11] A. A. Patel, D. Chowdhury, A. Allais, and S. Sachdev, "Confinement transition to density wave order in metallic doped spin liquids," Phys. Rev. B **93**, 165139 (2016), arXiv:1602.05954 [cond-mat.str-el].

[12] ITensor library v1.2.0, `http://itensor.org/`.

[13] S. R. White, D. J. Scalapino, and S. A. Kivelson, "One Hole in the Two-Leg t-J Ladder and Adiabatic Continuity to the Noninteracting Limit," Phys. Rev. Lett. **115**, 056401 (2015), arXiv:1502.04403 [cond-mat.str-el].

[14] J. Motruk, M. P. Zaletel, R. S. K. Mong, and F. Pollmann, "Density matrix renormalization group on a cylinder in mixed real and momentum space," Phys. Rev. B **93**, 155139 (2016), arXiv:1512.03318 [cond-mat.str-el].

[15] P. Calabrese and J. Cardy, "Entanglement entropy and quantum field theory," Journal of Statistical Mechanics: Theory and Experiment **6**, 06002 (2004), hep-th/0405152.

[16] P. Calabrese, M. Campostrini, F. Essler, and B. Nienhuis, "Parity Effects in the Scaling of Block Entanglement in Gapless Spin Chains," Phys. Rev. Lett. **104**, 095701 (2010), arXiv:0911.4660 [cond-mat.stat-mech].

[17] I. Affleck and A. W. W. Ludwig, "Universal noninteger "ground-state degeneracy" in critical quantum systems," Phys. Rev. Lett. **67**, 161 (1991).

[18] M. Rodney, H. F. Song, S.-S. Lee, K. Le Hur, and E. S. Sørensen, "Scaling of entanglement entropy across Lifshitz transitions," Phys. Rev. B **87**, 115132 (2013), arXiv:1210.8403 [cond-mat.str-el].

[19] A. Paramekanti and A. Vishwanath, "Extending Luttinger's theorem to $\mathbb{Z}_2$ fractionalized phases of matter," Phys. Rev. B **70**, 245118 (2004), cond-mat/0406619.